

Article

# Ionic Liquids as Grease Base Liquids

Robert Mozes <sup>1,†</sup>, Peter K. Cooper <sup>2,†</sup>, Rob Atkin <sup>2,\*</sup> and Hua Li <sup>2,\*</sup> 

<sup>1</sup> Priority Research Centre for Advanced Fluids and Interfaces, University of Newcastle, Callaghan, NSW 2308, Australia; robert.mozes@uon.edu.au

<sup>2</sup> School of Molecular Sciences, University of Western Australia, 35 Stirling Highway, Perth, WA 6009, Australia; peter.cooper@research.uwa.edu.au

\* Correspondence: rob.atkin@uwa.edu.au (R.A.); hua.li@uwa.edu.au (H.L.); Tel.: +61-8-648-84410 (R.A.); +61-8-648-85399 (H.L.)

† These authors contributed equally to this work.

Received: 10 July 2017; Accepted: 4 August 2017; Published: 8 August 2017

**Abstract:** The rheological characteristics of one mineral oil and two ionic liquid (IL) based lubricating greases were explored as a function of thickener concentration. The ILs used are 1-butyl-3-methylimidazolium bis(trifluoromethylsulfonyl)imide ([BMIM][TFSI]) and trihexyltetradecylphosphonium bis(trifluoromethylsulfonyl)imide ([P<sub>6,6,6,14</sub>][TFSI]), with polytetrafluoroethylene (PTFE) particles used as thickeners. Greases with different base liquid concentrations (60–80 wt %) were investigated using small-amplitude oscillatory shear and viscous flow measurements, and contact angle measurements probed adhesion at base liquid–PTFE interfaces. Rheological properties are influenced by base liquid–PTFE adhesion and the chemical structure of the grease base liquids. With the addition of thickener, the greases generally have higher elasticity, strain resistance, and frequency independent properties. Viscometric rheological tests illustrate non-Newtonian shear-thinning behaviour for all greases. [BMIM][TFSI] based greases show the most elastic properties and strain resistance, as well as the highest initial and lowest final viscosities of the greases tested.

**Keywords:** ionic liquids; lubricating grease; rheology

## 1. Introduction

Lubricating greases are multiphase systems composed of two main components: base liquids and thickeners. The base liquid, generally either a mineral or synthetic oil, acts as the lubricating substance that is bled from the grease structure. The thickener is either an emulsifying soap (e.g., lithium hydroxystearate) or powdered solid (e.g., polytetra-fluoroethylene (PTFE) particles) which acts to produce the semi-solid behavior of the grease. Grease thickeners form a three-dimensional gelation network (microstructure) which traps the oil and confers the appropriate rheological and tribological behavior to the grease [1]. Additives are frequently included to improve properties such as thermal or evaporative stability.

Viscoelasticity is the simultaneous presentation of both solid and liquid properties. It is a common characteristic that can be obtained by rheological measurements; however, this property becomes particularly prominent when assessing colloidal systems, including grease. The two main values used to describe viscoelasticity are the storage ( $G'$ ) and loss ( $G''$ ) moduli, which relate to the material's ability to store and dissipate energy, respectively. In a measurement, the storage modulus is often used as a measure of a material's elasticity, whilst the loss modulus is used to describe the viscous behavior.

The viscoelastic behavior of a grease is tuned by altering the thickener concentration, and thus the gelation network of the grease. Greases with high gelation levels have high resistance to flow, while still readily shear thinning at designated shear rate or stress. Yeong et al. [2] investigated the rheology

of lithium 12-hydroxystearate dispersions in mineral oil. At low thickener concentrations, the gelation network is not sufficiently developed to respond elastically over the frequencies tested. Increasing the thickener content to 6 wt % increases gelation which resists the constant angular deformation from long to short time steps. At higher thickener concentrations (10–14 wt %), the grease resists deformation over the entire range of time steps and is almost independent of the oscillating strain frequency. This demonstrates the thickener concentration can be used to achieve an appropriate level of gelation for the required application.

Ionic liquids (ILs) are salts with melting points below 100 °C. Low melting points are achieved by making at least one of the ions large and asymmetric which weakens electrostatic interactions and hinders packing into a crystal lattice [3].

Many ILs have properties which make them of high scientific interest, such as negligible vapor pressure, non-flammability, excellent solvency, wide electrochemical window, and chemical and thermal inertness [4,5]. For these reasons, ILs have been pursued as promising candidates in many fields such as catalysis [6–8], organic synthesis [9–11], electrochemistry [12–14] and spectroscopy [15–17].

There has been a surge of scientific interest in the application of ionic liquids as lubricants over the last ten years. A variety of ILs have been investigated as pure lubricants and lubricant additives at both macro- and nano-scales. For example, a commercially available IL, [BMIM][TFSI], has been tribologically assessed as a pure lubricating oil [18]. Compared to commercial lubricating oils of similar viscosities, this IL shows significantly improved friction coefficient and thermal stability. Studies from our group and others have shown that  $[P_{6,6,6,14}]^+$  cation based ILs are potential additives for hydrocarbon base oils for a variety of surfaces [19–27]. As little as 2 mol% IL dissolved in a base oil lubricates as effectively as the pure IL, and low concentration IL–oil mixtures are much more effective lubricants than the pure base oil [20–22], or oils with traditional additives [22,28].

For greases, ILs are excellent base liquid candidates, as their unusual physical properties can impart performance advantaged over traditional hydrocarbon oils. Only a few studies have investigated the tribology of IL based greases; the results showed better friction reduction and anti-wear properties than commercially available mineral oil based greases at both room and elevated temperatures [29–32]. However, no rheological study has been taken on IL based lubricating greases, so the viscoelasticity, deformation and flow properties under shear is unknown, which restricts translation IL based lubricating greases to automotive applications, such as ball and journal bearings. In this work, we investigate the rheology of two IL based lubricating greases, and contrast with a mineral oil based grease. The chemical structures of the ILs used in this study are presented in Figure 1. The  $[BMIM]^+$  and  $[P_{6,6,6,14}]^+$  cations and the [TFSI] anion have been chosen due to their stable properties in air and under shear [18,33–37]. As  $[BMIM]^+$  has more localized charges and shorter alkyl chains than  $[P_{6,6,6,14}]^+$ , the effect of the chemical structure of the cation on grease rheology is revealed.

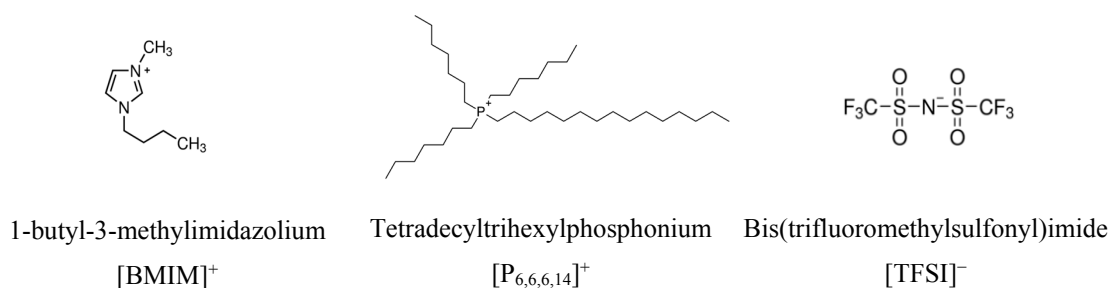


**Figure 1.** The chemical structure of Ionic Liquids used in this work.

## 2. Experimental

### 2.1. Materials

The mineral oil, acetone and 1  $\mu\text{m}$  PTFE particles were purchased from Sigma-Aldrich (St. Louis, MO, USA). [BMIM][TFSI] and [P<sub>6,6,6,14</sub>][TFSI] were purchased from IoLiTec (Heilbronn, Germany).

### 2.2. Methodology

#### 2.2.1. Contact Angle

The contact angles of the mineral oil and the ILs on a PTFE surface were measured via sessile drop test using an OCA10 tensiometer (Data Physics, Filderstadt, Germany). The contact angle of each droplet was measured three times and two droplets for each base liquid were analyzed. The mean values of the contact angles are listed in Table 1; the errors are within 10%.

**Table 1.** The contact angle and surface tension of mineral oil and the two ionic liquids.

Base Liquid	Contact Angle (°)	Surface Tension (mN/m)
Mineral Oil	27	26.1–29.3 [38]
[P <sub>6,6,6,14</sub> ][TFSI]	50	30.9 [39]
[BMIM][TFSI]	83	32.9 [40]

#### 2.2.2. Rheology

An AR G2 rheometer with attached peltier plate from TA Instruments was used to assess the rheology of the greases. The geometry used was a 2° stainless steel cone with a diameter of 40 mm.

Greases were prepared at ratios of 60, 70 and 80 wt % pure base liquid to PTFE. These concentrations were chosen as sufficiently “thick” greases form at these concentrations. Higher base oil concentrations lead to thinner greases with lower critical strains and modulus values. This means that tests would have to be performed at lower strain rates, increasing the experimental error. Further, the interactions of the storage and loss moduli become less pronounced as the concentration decreases and the materials become less viscoelastic. At lower base oil concentrations, the differences inherent in the greases produced by each of the base oils become less pronounced as the majority of the grease is made of the constant thickener rather than the base oil variable. Also, the greases become unrealistically thick, approaching putties rather than a workable grease.

Acetone equivalent to half the mass of the PTFE thickener was added to aid dispersion. The mixture was then homogenized via magnetic stirrer and the acetone was boiled out.

For the oscillatory strain sweep, the angular frequency was controlled at 10 s<sup>-1</sup> over the sweep from 0.01 to 100 strain %. For the oscillatory angular frequency sweep, the strain % was controlled at 0.10 from 1 to 400 rad·s<sup>-1</sup>. For the viscometric test, the shear rate was ramped from 0.001 to 1000 s<sup>-1</sup>. All runs were conditioned at a shear rate of 100 s<sup>-1</sup> for 60 s, followed by 300 s of equilibration time. All runs were performed in triplicate, with replacement of the grease between each run. The errors are within 10%; the data points in all plots are the average values.

## 3. Results and Discussion

### 3.1. Contact Angle

Sessile drop contact angle measurements were performed for the mineral oil and the two ILs on a PTFE surface. The contact angles are listed in Table 1, as well as literature values for surface tension.

The contact angle of a liquid is generally proportional to its surface tension according to Young’s equation when the solid surface tension and solid–liquid interfacial tension do not change significantly. As expected, the trend of the experimentally obtained contact angle values (mineral oil < [P<sub>6,6,6,14</sub>][TFSI]

< [BMIM][TFSI] is in line with the surface tension values of the base liquids in literature (Mineral Oil < [P<sub>6,6,6,14</sub>][TFSI] < [BMIM][TFSI]).

### 3.2. Rheological Testing

The viscoelasticity and deformation of the greases were explored by oscillatory rheological tests. The storage ( $G'$ ) and loss ( $G''$ ) moduli as a function of strain are obtained, as presented in Figure 2.

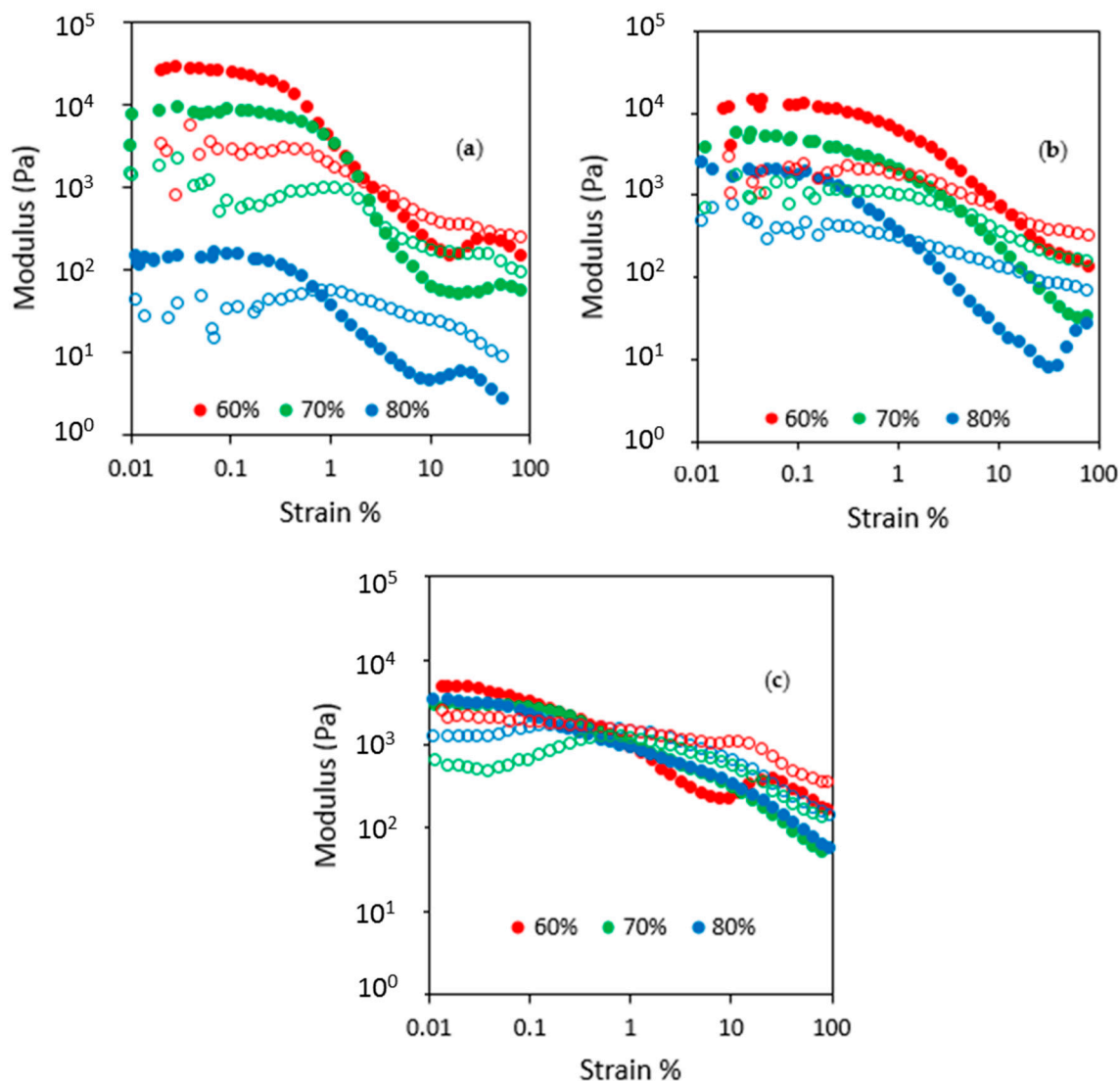


**Figure 2.** The storage ( $G'$ ) and loss modulus ( $G''$ ) vs strain % for (a) mineral oil; (b) [BMIM] [TFSI] and (c) [P<sub>6,6,6,14</sub>] [TFSI] based greases. Greases tested are composed of 60, 70 and 80 wt % base oil utilizing a PTFE thickener. Closed circles indicate storage modulus, whilst open circles indicate loss modulus values.

#### 3.2.1. Strain Sweep

A grease is capable of resisting small strains in an elastic fashion. All grease systems investigated in this study show an initial resistance, which is a plateau of the storage modulus ( $G'$ ) at low strain % in Figure 2, referred to as the linear viscoelastic region (LVR). When the stress is higher than the yield stress, the grease starts to bleed the base liquid, resulting in a dampened elastic response. The transition point between these two regimes is labelled as the critical strain, which is the onset of a reduction in the storage modulus with strain and the end of the LVR region. The ratio of the loss to storage moduli

is described by the  $\tan(\delta)$  value and can be subjectively correlated to physical characteristics of the grease such as fluidity and elasticity. Small  $\tan(\delta)$  ( $<1$ ) means the grease is solid-like and large  $\tan(\delta)$  ( $>1$ ) means the grease is liquid-like. The intersection of the steeply decreasing storage modulus with the loss modulus as strain increases is determined to be the point at which the grease microstructure has broken down. Physically, this represents the transition from a solid-like to a liquid-like state [41]. The critical strain, the average  $\tan(\delta)$  in the LVR region and the moduli intersection for each of the greases are presented in Table 2.

**Table 2.** Critical strain, average linear viscoelastic region (LVR)  $\tan(\delta)$  and storage loss moduli intersection of each grease obtained from oscillatory strain sweep.

Base Liquid	Base Liquid Concentration (wt %)	Critical Strain (Strain %)	Average LVR $\tan(\delta)$ (Dimensionless)	Moduli Intersection (Strain %)
Mineral Oil	60	0.27	0.121	2.76
	70	0.16	0.142	3.02
	80	0.072	0.229	0.751
[BMIM] [TFSI]	60	0.85	0.179	13.4
	70	0.66	0.269	4.40
	80	0.21	0.334	1.37
[P <sub>6,6,6,14</sub> ] [TFSI]	60	0.33	0.564	0.482
	70	0.26	0.257	0.670
	80	0.17	0.524	0.199

The storage and loss moduli values for all three greases strongly depend on base liquid concentration. An increase in the base liquid wt % results in the reduction of both modulus values. However, the extent of modulus reduction is significantly different for the three grease families. When the concentration of mineral oil increases from 60 wt % to 80 wt %, both storage and loss moduli values in the LVR region decrease by more than two orders of magnitude, whereas this drop for [BMIM][TFSI] based greases is less than one order of magnitude, and for [P<sub>6,6,6,14</sub>][TFSI] is even less significant. Thus, although at the low base liquid concentration of 60 wt %, mineral oil based grease shows highest  $G'$  and  $G''$ ; it shows lowest moduli values at 80 wt %, which means mineral oil based grease is not as stable as the two IL based greases at high base liquid concentrations. This does not follow the contact angle and surface tension trends presented in Table 1, revealing the moduli values and their dependence on base liquid concentration are likely influenced by base liquid properties other than PTFE wetting properties.

All greases have  $\tan(\delta)$  values lower than 1 in LVR region (cf. Table 2) and can, thus, be described as solid-like structures at rest. Mineral oil greases consistently demonstrate lowest  $\tan(\delta)$  values at low strain %, followed by [BMIM][TFSI] and [P<sub>6,6,6,14</sub>][TFSI]. Decreasing base liquid wt % and thus increasing thickener wt % corresponds to decreasing values of  $\tan(\delta)$ . This indicates that increasing thickener content produces a more extensive gelation network that is capable of exhibiting more pronounced elastic properties [1].

The wetting properties of the base liquid with the particle thickeners, described in this study using contact angles, were expected to be a major factor in both the solidity and stress resistance. A base liquid with low contact angle on a PTFE surface has a high work of adhesion which is the reversible work per unit area required to separate the liquid from the solid [42], thus the grease made from this base liquid is expected to be more stable and have high shear resistance, including wider LVR region and higher critical strain. However, the critical strain shown in Table 2 increases with contact angle, which is opposite to what is expected. Further, there seems to be no direct correlation between the linear viscoelastic region storage modulus,  $\tan(\delta)$  or moduli intersection presented in Table 2 and the contact angle values shown in Table 1. These results suggest that besides simple adhesions between base liquids and particles, other factors, such as base liquid chemical structure, have on these viscoelastic properties.

Greases with higher moduli intersection generally have a stronger microstructure [41]. Table 2 therefore indicates that [BMIM][TFSI] based greases have the strongest microstructure, followed by mineral oil based greases, and [P<sub>6,6,6,14</sub>][TFSI] based greases the weakest microstructure. These results are likely related to the structure and properties of the base liquids. The [BMIM] cation is relatively small and stiff with a higher charge density when compared to [P<sub>6,6,6,14</sub>], which is large and the charge is shielded by the long and branched alkyl chains. This leads to more ordered packing of [BMIM][TFSI] than [P<sub>6,6,6,14</sub>][TFSI] on PTFE particles, as previously seen in other surfaces [20,43], which leads to a more robust grease microstructure and increased resistance to strain. Mineral oil has lower interfacial tension than [P<sub>6,6,6,14</sub>][TFSI], so more energy is required to separate the base liquid and the thickener particles to break the microstructure. The fact that [BMIM][TFSI] shows better strain resistance than mineral oil indicates that the interactions of PTFE particles with [BMIM]<sup>+</sup> cations in [BMIM][TFSI] are stronger than with alkane molecules in the mineral oils.

### 3.2.2. Angular Frequency Sweep

The storage and loss moduli as a function of angular frequency are shown in Figure 2. The angular frequency sweeps were performed at a constant strain of 0.1%, beneath the critical strain, and therefore within the LVR region for all greases.

As with the strain sweep data presented in Figure 2, the magnitude of the moduli in Figure 3 is strongly dependent on the base liquid concentration. For all greases tested, increasing the thickener content results in an increase in both the storage and loss moduli. This is consistent with previous observation that increased thickener content leads to more extensive gelation, and a stronger microstructure.

The angular frequency sweeps in Figure 3 show that at low angular frequency  $G'$  and  $G''$  run parallel, with  $G'$  dominating  $G''$  for mineral oil and [BMIM][TFSI] based greases. This parallel angular frequency sweep represents an approximation of the LVR conditions at steady state, as low frequencies correspond to longer time steps for constant angular deformation [44]. As frequency increases, greases exhibiting strong microstructure will tend to continue the frequency independent parallel trend, as seen for 60 wt % and 70 wt % data for [BMIM][TFSI] and mineral oil. When the base liquid concentration increases to 80 wt %, the storage and loss moduli become similar at higher angular frequency for both [BMIM][TFSI] and mineral oil, indicating a weaker grease microstructure. The time step decrease at high angular frequency results in a departure from the steady state and causes weaker gel networks to succumb to structural breakdown. This prompts an increase in the moduli, with  $G''$  affected more significantly. The storage and loss moduli for all [P<sub>6,6,6,14</sub>][TFSI] based greases cross each other at an angular frequency ~50 rad/s (Figure 3c). These results suggest that [BMIM][TFSI] and mineral oil have a stronger microstructure than [P<sub>6,6,6,14</sub>][TFSI], at least when the base liquid is 60 wt % and 70 wt %, which is in line with the strain sweep results.

### 3.2.3. Viscous Response to Shear

Greases are non-Newtonian fluids with pseudoplastic characteristics. The initial and final viscosity data of the greases is presented in Table 3. At the initial state, the shear rate is very low, greases act in a semi-solid manner, leading to high initial viscosities. As shear increases, the yield stress is eventually exceeded. At this point, the microstructure begins to break apart. This releases, or 'bleeds', the base liquid onto the interface causing the viscosity to reduce rapidly until a minimum viscosity is reached [41]. This process is effectively showcased in Figure 4. All greases, excluding 60 wt % [BMIM][TFSI], present high initial viscosity, with a sharp decrease as shear rate rises and a retarding rate of decline at the maximum shear, indicative of a plateau in the region. As such, their minimum viscosity is assumed to be their final viscosity.

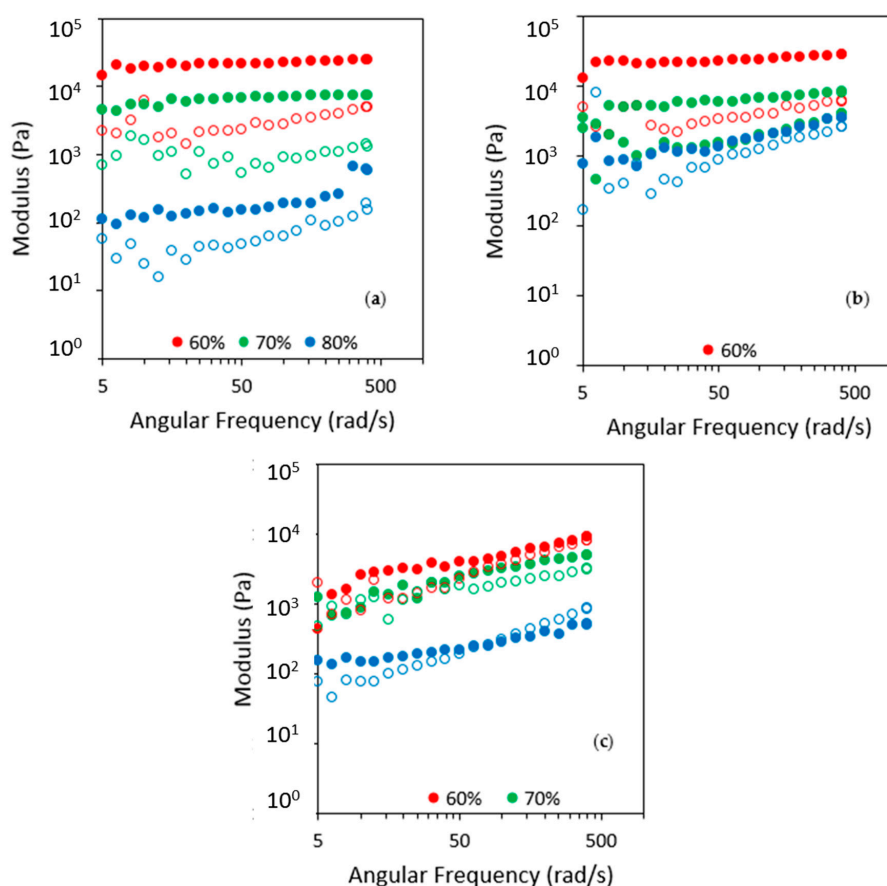


**Figure 3.** The storage ( $G'$ ) and loss modulus ( $G''$ ) vs Angular Frequency for (a) mineral oil; (b) [BMIM][TFSI] and (c) [P<sub>6,6,6,14</sub>][TFSI] based greases. Greases tested are composed of 60, 70 and 80 wt % base liquid utilizing a PTFE thickener. Closed circles present storage modulus; open circles present loss modulus.

In Figure 4b, the 60 wt % [BMIM][TFSI] grease demonstrates a peculiar trend towards the end of the run. Unlike the other samples, which tend to plateau by the end of the run, this grease began deviating downwards from the expected trend at approximately  $10 \text{ s}^{-1}$ . The final viscosity achieved by this grease ( $1.05 \times 10^{-3} \text{ Pa}\cdot\text{s}$ ) is significantly less than the viscosity of the base liquid ( $50.6 \times 10^{-3} \text{ Pa}\cdot\text{s}$ ) without thickener. This indicates that this IL shows a more significant shear thinning behavior than other liquids tested, perhaps due differences in liquid nanostructure as seen in previous studies [45–47].

**Table 3.** Critical viscometric data for the greases studied.

Base Liquid	Base Liquid Viscosity (mPa·s)	Base Liquid Concentration (wt %)	Initial Viscosity $10^3$ (Pa·s)	Final Viscosity $10^{-3}$ (Pa·s)
Mineral Oil	15.0 [48]	60	24.3	227
		70	11.2	251
		80	2.09	86.7
[BMIM][TFSI]	50.6 [49]	60	103	1.05
		70	43.6	147
		80	15.1	196
[P <sub>6,6,6,14</sub> ][TFSI]	43.8 [39]	60	40.3	423
		70	6.18	1050
		80	7.54	1210

The initial viscosity of every grease decreases with base liquid concentration, except for 70%  $[P_{6,6,6,14}][TFSI]$ . However, the trend for the final viscosity is different. For mineral oil, the final viscosity generally decreases with the increase of base liquid concentration due to weakening of the grease gel network and microstructure. For  $[BMIM][TFSI]$  and  $[P_{6,6,6,14}][TFSI]$ , the trend is opposite, with the final viscosity increasing with base liquid concentration. The reason for this is not clear yet, and may be due to the high IL concentration leading to a more robust grease microstructure than mineral oils of the same concentration. This is the topic of continued study.

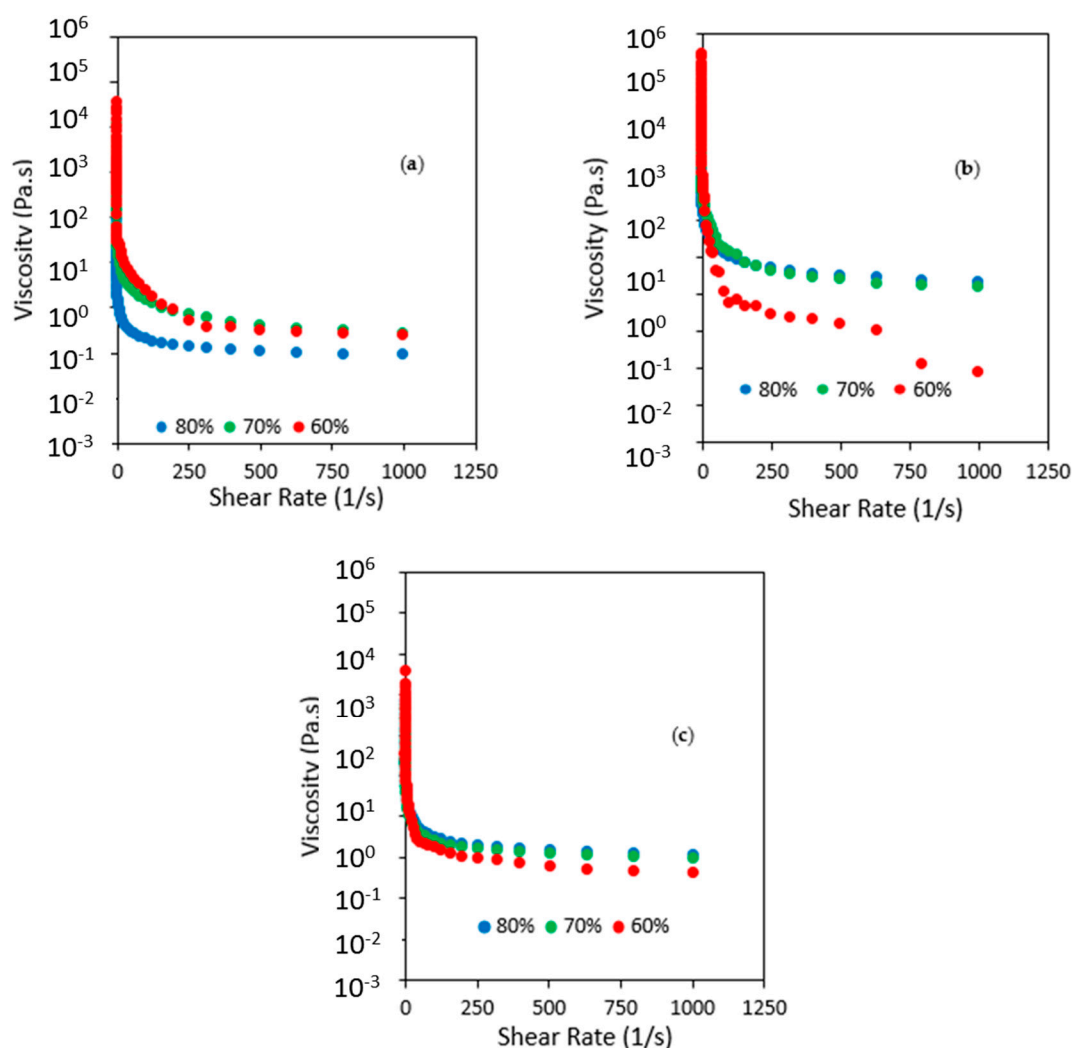


**Figure 4.** Viscosity as a function of shear rate for (a) mineral oil; (b)  $[BMIM][TFSI]$  and (c)  $[P_{6,6,6,14}][TFSI]$  based greases at base liquid concentrations of 60, 70 and 80 wt %.

Rheological traits suggest suitable greases for applications. High initial viscosity allows for simpler storage and transportation, whilst low minimum viscosity reduces hydrodynamic energy dissipation for ball and journal bearings, etc., resulting in energy and economic savings. Therefore,  $[BMIM][TFSI]$  exhibits the most valuable viscometric properties by possessing both the highest initial and lowest final viscosity.

#### 4. Conclusions

The rheology of greases made from different base liquids (mineral oil,  $[BMIM][TFSI]$  and  $[P_{6,6,6,14}][TFSI]$ ) was investigated at 60, 70 and 80 wt % base liquid concentrations.

Oscillatory strain analysis reveals the microstructural strength, linear viscoelastic region and deformation resistance of the greases. The storage modulus, critical strain and moduli intersection are influenced by the base liquid chemical structure and interfacial properties, i.e., surface tension. [BMIM][TFSI] significantly outperforms [P<sub>6,6,6,14</sub>][TFSI] in all tests. It has a high critical yield, high modulus intersection and low average LVR  $\tan(\delta)$  values. Oscillatory angular frequency analysis was utilized to define the viscoelastic behavior of the greases. [BMIM][TFSI] and mineral oil based greases with low base liquid concentrations demonstrate angular frequency independence, indicative of strong gelation network. The moduli dependence on angular frequency is more significant for high base liquid concentration [BMIM][TFSI] and mineral oil greases and all [P<sub>6,6,6,14</sub>][TFSI] based greases, which implies grease microstructural breakdown in these conditions.

Viscometric analysis was performed to elucidate the greases' viscous responses to a range of applied shear rates. The initial viscosities of the greases are in the same trend with the base liquids, with [BMIM][TFSI] the highest, [P<sub>6,6,6,14</sub>][TFSI] second and mineral oil the lowest. However, the final viscosity is different ([P<sub>6,6,6,14</sub>][TFSI] > mineral oil > [BMIM][TFSI]), suggesting IL base liquids can produce unexpected shear thinning effects.

**Acknowledgments:** Peter K. Cooper would like to thank The University of Western Australia and The Australian Research Council for providing a Research Training Program scholarship.

**Author Contributions:** Robert Mozes, Peter K. Cooper, Hua Li and Rob Atkin conceived and designed the experiments; Robert Mozes and Peter K. Cooper performed the experiments; Robert Mozes, Peter K. Cooper, Hua Li and Rob Atkin analyzed the data; Robert Mozes, Peter K. Cooper, Hua Li and Rob Atkin wrote the paper.

**Conflicts of Interest:** The authors declare no conflict of interest.

## References

- Roman, C.; Valencia, C.; Franco, J.M. AFM and SEM Assessment of Lubricating Grease Microstructures: Influence of Sample Preparation Protocol, Frictional Working Conditions and Composition. *Tribol. Lett.* **2016**, *63*, 20. [[CrossRef](#)]
- Yeong, S.K.; Luckham, P.F.; Tadros, T.F. Steady flow and viscoelastic properties of lubricating grease containing various thickener concentrations. *J. Colloid Interface Sci.* **2004**, *274*, 285–293. [[CrossRef](#)] [[PubMed](#)]
- Hayes, R.; Warr, G.G.; Atkin, R. At the Interface: Solvation and Designing Ionic Liquids. *Phys. Chem. Chem. Phys.* **2010**, *12*, 1709–1723. [[CrossRef](#)] [[PubMed](#)]
- Hagiwara, R.; Ito, Y. Room temperature ionic liquids of alkyimidazolium cations and fluoroanions. *J. Fluor. Chem.* **2000**, *105*, 221–227. [[CrossRef](#)]
- Huddleston, J.G.; Visser, A.E.; Reichert, W.M.; Willauer, H.D.; Broker, G.A.; Rogers, R.D. Characterization and comparison of hydrophilic and hydrophobic room temperature ionic liquids incorporating the imidazolium cation. *Green Chem.* **2001**, *3*, 156–164. [[CrossRef](#)]
- Gordon, C.M. New developments in catalysis using ionic liquids. *Appl. Catal. A Gen.* **2001**, *222*, 101–117. [[CrossRef](#)]
- Welton, T. Ionic liquids in catalysis. *Coord. Chem. Rev.* **2004**, *248*, 2459–2477. [[CrossRef](#)]
- Zhao, D.; Wu, M.; Kou, Y.; Min, E. Ionic liquids: Applications in catalysis. *Catal. Today* **2002**, *74*, 157–189. [[CrossRef](#)]
- Azizi, N.; Shirdel, F. Task specific dicationic acidic ionic liquids catalyzed efficient and rapid synthesis of benzoxanthenones derivatives. *J. Mol. Liq.* **2016**, *222*, 783–787. [[CrossRef](#)]
- Fischer, T.; Sethi, A.; Welton, T.; Woolf, J. Diels-Alder reactions in room-temperature ionic liquids. *Tetrahedron Lett.* **1999**, *40*, 793–796. [[CrossRef](#)]
- Vafaezadeh, M.; Alinezhad, H. Brønsted acidic ionic liquids: Green catalysts for essential organic reactions. *J. Mol. Liq.* **2016**, *218*, 95–105. [[CrossRef](#)]
- De Souza, R.F.; Padilha, J.C.; Gonçalves, R.S.; Dupont, J. Room temperature dialkyimidazolium ionic liquid-based fuel cells. *Electrochem. Commun.* **2003**, *5*, 728–731. [[CrossRef](#)]
- Galiński, M.; Lewandowski, A.; Stępnia, I. Ionic liquids as electrolytes. *Electrochim. Acta* **2006**, *51*, 5567–5580. [[CrossRef](#)]

14. Garcia, B.; Lavallée, S.; Perron, G.; Michot, C.; Armand, M. Room temperature molten salts as lithium battery electrolyte. *Electrochim. Acta* **2004**, *49*, 4583–4588. [[CrossRef](#)]
15. Liu, J.-F.; Jiang, G.-B.; Liu, J.-F.; Jönsson, J.Å. Application of ionic liquids in analytical chemistry. *TrAC Trends Anal. Chem.* **2005**, *24*, 20–27. [[CrossRef](#)]
16. Pandey, S. Analytical applications of room-temperature ionic liquids: A review of recent efforts. *Anal. Chim. Acta* **2006**, *556*, 38–45. [[CrossRef](#)] [[PubMed](#)]
17. Sun, P.; Armstrong, D.W. Ionic liquids in analytical chemistry. *Anal. Chim. Acta* **2010**, *661*, 1–16. [[CrossRef](#)] [[PubMed](#)]
18. Mordukhovich, G.; Qu, J.; Howe, J.Y.; Bair, S.; Yu, B.; Luo, H.; Smolenski, D.J.; Blau, P.J.; Bunting, B.G.; Dai, S. A low-viscosity ionic liquid demonstrating superior lubricating performance from mixed to boundary lubrication. *Wear* **2013**, *301*, 740–746. [[CrossRef](#)]
19. Yu, B.; Bansal, D.G.; Qu, J.; Sun, X.; Luo, H.; Dai, S.; Blau, P.J.; Bunting, B.G.; Mordukhovich, G.; Smolenski, D.J. Oil-miscible and non-corrosive phosphonium-based ionic liquids as candidate lubricant additives. *Wear* **2012**, *289*, 58–64. [[CrossRef](#)]
20. Li, H.; Cooper, P.K.; Somers, A.E.; Rutland, M.W.; Howlett, P.C.; Forsyth, M.; Atkin, R. Ionic Liquid Adsorption and Nanotribology at the Silica–Oil Interface: Hundred-Fold Dilution in Oil Lubricates as Effectively as the Pure Ionic Liquid. *J. Phys. Chem. Lett.* **2014**, *5*, 4095–4099. [[CrossRef](#)] [[PubMed](#)]
21. Li, H.; Somers, A.E.; Howlett, P.C.; Rutland, M.W.; Forsyth, M.; Atkin, R. Addition of low concentrations of an ionic liquid to a base oil reduces friction over multiple length scales: A combined nano-and macrotribology investigation. *Phys. Chem. Chem. Phys.* **2016**, *18*, 6541–6547. [[CrossRef](#)] [[PubMed](#)]
22. Li, H.; Somers, A.E.; Rutland, M.W.; Howlett, P.C.; Atkin, R. Combined Nano- and Macrotribology Studies of Titania Lubrication Using the Oil-Ionic Liquid Mixtures. *ACS Sustain. Chem. Eng.* **2016**, *4*, 5005–5012. [[CrossRef](#)]
23. Somers, A.; Yunis, R.; Armand, M.; Pringle, J.; MacFarlane, D.; Forsyth, M. Towards Phosphorus Free Ionic Liquid Anti-Wear Lubricant Additives. *Lubricants* **2016**, *4*, 22. [[CrossRef](#)]
24. Somers, A.E.; Khemchandani, B.; Howlett, P.C.; Sun, J.; MacFarlane, D.R.; Forsyth, M. Ionic Liquids as Antiwear Additives in Base Oils: Influence of Structure on Miscibility and Antiwear Performance for Steel on Aluminum. *ACS Appl. Mater. Interfaces* **2013**, *5*, 11544–11553. [[CrossRef](#)] [[PubMed](#)]
25. Qu, J.; Barnhill, W.C.; Luo, H.; Meyer, H.M.; Leonard, D.N.; Landauer, A.K.; Kheireddin, B.; Gao, H.; Papke, B.L.; Dai, S. Synergistic Effects Between Phosphonium-Alkylphosphate Ionic Liquids and Zinc Dialkyldithiophosphate (ZDDP) as Lubricant Additives. *Adv. Mater.* **2015**, *27*, 4767–4774. [[CrossRef](#)] [[PubMed](#)]
26. Qu, J.; Meyer, H.M.; Cai, Z.-B.; Ma, C.; Luo, H. Characterization of ZDDP and ionic liquid tribofilms on non-metallic coatings providing insights of tribofilm formation mechanisms. *Wear* **2015**, *332–333*, 1273–1285. [[CrossRef](#)]
27. Elbourne, A.; Sweeney, J.; Webber, G.B.; Wanless, E.J.; Warr, G.G.; Rutland, M.W.; Atkin, R. Adsorbed and near-surface structure of ionic liquids determines nanoscale friction. *Chem. Commun.* **2013**, *49*, 6797–6799. [[CrossRef](#)] [[PubMed](#)]
28. Qu, J.; Luo, H.; Chi, M.; Ma, C.; Blau, P.J.; Dai, S.; Viola, M.B. Comparison of an oil-miscible ionic liquid and ZDDP as a lubricant anti-wear additive. *Tribol. Int.* **2014**, *71*, 88–97. [[CrossRef](#)]
29. Fan, X.; Xia, Y.; Wang, L. Tribological properties of conductive lubricating greases. *Friction* **2014**, *2*, 343–353. [[CrossRef](#)]
30. Wang, Z.; Xia, Y.; Liu, Z.; Wen, Z. Conductive Lubricating Grease Synthesized Using the Ionic Liquid. *Tribol. Lett.* **2012**, *46*, 33–42. [[CrossRef](#)]
31. Cai, M.; Liang, Y.; Zhou, F.; Liu, W. Tribological Properties of Novel Imidazolium Ionic Liquids Bearing Benzotriazole Group as the Antiwear/Anticorrosion Additive in Poly(ethylene glycol) and Polyurea Grease for Steel/Steel Contacts. *ACS Appl. Mater. Interfaces* **2011**, *3*, 4580–4592. [[CrossRef](#)] [[PubMed](#)]
32. Cai, M.; Zhao, Z.; Liang, Y.; Zhou, F.; Liu, W. Alkyl Imidazolium Ionic Liquids as Friction Reduction and Anti-Wear Additive in Polyurea Grease for Steel/Steel Contacts. *Tribol. Lett.* **2010**, *40*, 215–224. [[CrossRef](#)]
33. Kheireddin, B.A.; Lu, W.; Chen, I.C.; Akbulut, M. Inorganic nanoparticle-based ionic liquid lubricants. *Wear* **2013**, *303*, 185–190. [[CrossRef](#)]
34. Totolin, V.; Minami, I.; Gabler, C.; Dörr, N. Halogen-free borate ionic liquids as novel lubricants for tribological applications. *Tribol. Int.* **2013**, *67*, 191–198. [[CrossRef](#)]

35. Gabler, C.; Dörr, N.; Allmaier, G. Influence of cationic moieties on the tribolayer constitution shown for bis(trifluoromethylsulfonyl)imide based ionic liquids studied by X-ray photoelectron spectroscopy. *Tribol. Int.* **2014**, *80*, 90–97. [[CrossRef](#)]
36. Pisarova, L.; Totolin, V.; Gabler, C.; Dörr, N.; Pittenauer, E.; Allmaier, G.; Minami, I. Insight into degradation of ammonium-based ionic liquids and comparison of tribological performance between selected intact and altered ionic liquid. *Tribol. Int.* **2013**, *65*, 13–27. [[CrossRef](#)]
37. Monge, R.; González, R.; Hernández Battez, A.; Fernández-González, A.; Viesca, J.L.; García, A.; Hadfield, M. Ionic liquids as an additive in fully formulated wind turbine gearbox oils. *Wear* **2015**, *328–329*, 50–63. [[CrossRef](#)]
38. Mendonça, C.G.D.; Raetano, C.G.; Mendonça, C.G.D. Surface tension of mineral oils and vegetable oils. *Eng. Agrícola* **2007**, *27*, 16–23. [[CrossRef](#)]
39. Lago, S.; Rodríguez-Cabo, B.; Arce, A.; Soto, A. Water/oil/[P6,6,6,14][NTf2] phase equilibria. *J. Chem. Thermodyn.* **2014**, *75*, 63–68. [[CrossRef](#)]
40. Klomfar, J.; Součková, M.; Pátek, J. Surface tension measurements with validated accuracy for four 1-alkyl-3-methylimidazolium based ionic liquids. *J. Chem. Thermodyn.* **2010**, *42*, 323–329. [[CrossRef](#)]
41. Paszkowski, M. Some Aspects of Grease Flow in Lubrication Systems and Friction Nodes. In *Tribology—Fundamentals and Advancements*; Gegner, D.J., Ed.; InTech: Rijeka, Croatia, 2013.
42. Li, H.; Sedev, R.; Ralston, J. Dynamic wetting of a fluoropolymer surface by ionic liquids. *Phys. Chem. Chem. Phys.* **2011**, *13*, 3952–3959. [[CrossRef](#)] [[PubMed](#)]
43. Li, H.; Wood, R.J.; Endres, F.; Atkin, R. Influence of alkyl chain length and anion species on ionic liquid structure at the graphite interface as a function of applied potential. *J. Phys. Condens. Matter* **2014**, *26*, 284115. [[CrossRef](#)] [[PubMed](#)]
44. Dixena, R.; Sayanna, E.; Badoni, R. Recycled and Virgin HDPEs as Bleed Inhibitors and Their Rheological Influences on Lubricating Greases Thickened with PP and mPP. *Lubricants* **2014**, *2*, 237–248. [[CrossRef](#)]
45. Smith, J.A.; Webber, G.B.; Warr, G.G.; Atkin, R. Rheology of Protic Ionic Liquids and Their Mixtures. *J. Phys. Chem. B* **2013**, *117*, 13930–13935. [[CrossRef](#)] [[PubMed](#)]
46. Hayes, R.; Imberti, S.; Warr, G.G.; Atkin, R. Effect of Cation Alkyl Chain Length and Anion Type on Protic Ionic Liquid Nanostructure. *J. Phys. Chem. C* **2014**, *118*, 13998–14008. [[CrossRef](#)]
47. Elbourne, A.; Voitchovsky, K.; Warr, G.G.; Atkin, R. Ion structure controls ionic liquid near-surface and interfacial nanostructure. *Chem. Sci.* **2015**, *6*, 527–536. [[CrossRef](#)]
48. Mineral Oil. Available online: <http://www.sigmaaldrich.com/catalog/product/sial/330779?lang=en&region=AU> (accessed on 20 October 2016).
49. Tariq, M.; Carvalho, P.J.; Coutinho, J.A.P.; Marrucho, I.M.; Lopes, J.N.C.; Rebelo, L.P.N. Viscosity of (C2–C14) 1-alkyl-3-methylimidazolium bis(trifluoromethylsulfonyl)amide ionic liquids in an extended temperature range. *Fluid Phase Equilibria* **2011**, *301*, 22–32. [[CrossRef](#)]

